Bioinspired Adaptive Control for Artificial Muscles

Conference Paper · July 2013

DOI: 10.1007/978-3-642-39802-5_27

6 authors, including:

Emma Wilson
The University of Sheffield
16 PUBLICATIONS **29** CITATIONS
SEE PROFILE

Tareq Assaf
University of the West of England, Bristol
26 PUBLICATIONS **98** CITATIONS
SEE PROFILE

Sean R Anderson
The University of Sheffield
45 PUBLICATIONS **349** CITATIONS
SEE PROFILE

John Porrill
The University of Sheffield
132 PUBLICATIONS **2,738** CITATIONS
SEE PROFILE

Bioinspired Adaptive Control for Artificial Muscles

Emma D. Wilson[1], Tareq Assaf[2], Martin J. Pearson[2], Jonathan M. Rossiter[2], Sean R. Anderson[1], and John Porrill[1]

[1] Sheffield Centre for Robotics (SCentRo), University of Sheffield, UK
[2] Bristol Robotics Laboratory (BRL), University of the West of England and University of Bristol, UK

Abstract. The new field of soft robotics offers the prospect of replacing existing hard actuator technologies by artificial muscles more suited to human-centred robotics. It is natural to apply biomimetic control strategies to the control of these actuators. In this paper a cerebellar-inspired controller is successfully applied to the real-time control of a dielectric electroactive actuator. To analyse the performance of the algorithm in detail we identified a time-varying plant model which accurately described actuator properties over the length of the experiment. Using synthetic data generated by this model we compared the performance of the cerebellar-inspired controller with that of a conventional adaptive control scheme (filtered-x LMS). Both the cerebellar and conventional algorithms were able to control displacement for short periods, however the cerebellar-inspired algorithm significantly outperformed the conventional algorithm over longer duration runs where actuator characteristics changed significantly. This work confirms the promise of biomimetic control strategies for soft-robotics applications.

1 Introduction

The scalability, high mechanical compliance, structural simplicity, high versatility, proprioceptive feedback and large strain capability of biological muscle make it an excellent multi-purpose actuator [1]. As a result, there has been a major effort to develop actuator technologies capable of mimicking the performance of biological muscle [2]. Such artificial muscle actuators would be ideal for use in robots working in unstructured environments and for applications where safe human-robot interaction is required [3].

Electroactive polymers (EAPs) form a class of materials that are capable of undergoing large deformations in response to suitable electrical stimuli. They possess many of the desirable properties of biological muscle [4, 5]. There are two major classes of EAPs: dielectric and ionic. Here we consider the control of dielectric electroactive polymers (DEAs). DEAs can be used to manufacture compliant actuators with high energy density, large strain capability, a relatively fast response, and which have the capacity for self sensing [6–8].

N.F. Lepora et al. (Eds.): Living Machines 2013, LNAI 8064, pp. 311–322, 2013.

Current research into EAPs has focused on the development of new actuator configurations and materials to provide better actuation properties [9, 10]. Some effort has been made to investigate control strategies for ionic EAPs using adaptive inverse control [11, 12], model reference adaptive control [13], and PID feedback control [14]. There has been less focus on the control of DEAs, and much of what there is has used non-adaptive schemes such as PID controllers [6,10]. In fact DEAs present a number of interesting control challenges, for example they are manufactured with wide tolerances, and are subject to creep and time related ageing [6]. Although these characteristics of EAPs would seem to be well-suited to adaptive control methods there has been a gap in the development suitable techniques.

In this investigation we address the adaptive control problem for a DEA using a bioinspired approach. Although EAPs are commonly termed artificial muscles, as far as we are aware bioinspired adaptive control schemes have not yet been applied to EAPs. This is in spite of the clear similarity between EAPs and muscle in many of their control challenges [4]. Taking inspiration from the neuromuscular control system would seem to be a natural strategy since it has evolved to be well suited to adapting and tuning the control of a wide range of motor behaviours in unstructured, changing environments [3].

In this contribution we apply a bio-inspired framework based on the known properties of the cerebellum to the adaptive control of a DEA actuator. The cerebellum is a region of the brain strongly associated with adaptive control and skilled movement [20]. The basic cerebellar microcircuit has similar structure to an adaptive filter, which has been well established over numerous investigations [17–21]. Furthermore, cerebellar based control algorithms have previously been successfully applied to other robotic control applications [22–25]. In order to evaluate the performance of the cerebellar algorithm we benchmark it against a conventional adaptive control scheme (filtered-x LMS – FXLMS) [15] which has previously been applied to vibration isolation using a DEA actuator.

The paper is organised as follows. The control algorithms are described in Section 2 and experiment details are given in Section 3. Section 4 presents the results from experiments. These results include real time control of the DEA behaviour and the comparison with the performance of a conventional controller using a simulated DEA plant. Finally, the results are discussed in Section 5.

2 Adaptive Control Algorithms

A bio-inspired control scheme, based on the adaptive filter model of the cerebellum, will be compared to the FXLMS algorithm. The FXLMS algorithm was chosen as a benchmark because of its previous application to the adaptive control of a DEA [15]. The bio-inspired scheme uses an architecture originally studied in the context of the vestibular ocular reflex (VOR) [26]. This section describes the two algorithms, both of which are adaptive control schemes that use LMS to adjust the weights of an adaptive filter.

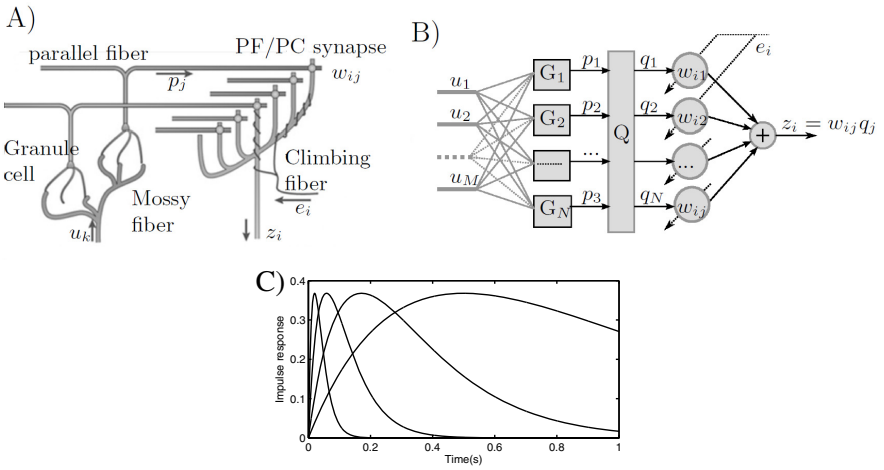

Fig. 1. A) Schematic of the basic cerebellar microcircuit showing granule cells, parallel fibres and a Purkinje cell (PC). B) Interpretation of the cerebellar microcircuit as an adaptive filter (including a Q-matrix optimisation in the granular layer to enable fast learning). Processing by the granule cells is modelled as a filter $p_j = G_j[u_1, u_2...]$, followed by signal decorrelation into signals q_j using a matrix Q. The Purkinje cell output takes a weighted sum of the inputs, q_j, where the filter weights are adjusted using the covariance learning rule. C) Normalised impulse responses of the four log-spaced α-function basis filters.

2.1 Cerebellar Algorithm

The cerebellar microcircuit can be modelled as an adaptive filter [17, 21], as illustrated in Figure 1. In the adaptive filter model of the cerebellum, initial processing in the granule cell layer is modelled as a bank of basis filters. In this contribution we model these basis as α-function filters, with Laplace transforms

$$G_k(s) = \frac{1}{(T_k s + 1)^2} \tag{1}$$

where T_k is the filter time constant. To control the DEA we use four log-spaced time constants between 0.02s and 0.5s (see Figure 1C). A constant filter implementing a bias term is also included. This α-basis replaces the tapped delay lines (TDLs) commonly used in engineering applications. This basis set provides a biologically plausible way of representing timing in which signals with larger delay are more dispersed in time, allowing a compact representation of phenomena on both fast and slow time-scales. It has been shown to greatly reduce the number of adaptable parameters required in comparison to using conventional TDLs [27, 28].

The filter outputs p_j are highly correlated, therefore a matrix Q is used to decorrelate these signals and speed up learning [29, 30], giving the signals q_j which are weighted and summed to give the cerebellar output. The weights w_{ij}

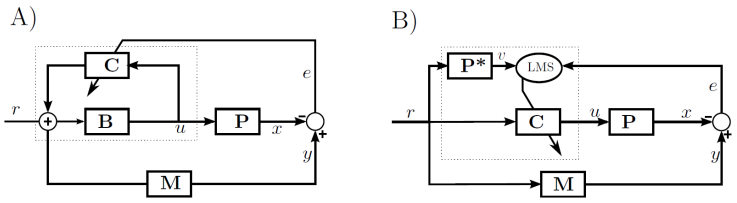

Fig. 2. The two adaptive control schemes (each controller is contained in a dotted box) used to learn to drive the output (x) of the DEA plant P to match a desired trajectory y. A) The cerebellar control architecture. The motor command is generated by a fixed element B, and an adaptive element C in a recurrent loop. B) Filtered-x LMS control. The motor command is generated by an adaptive filter C. The algorithm requires a model $P*$ of the plant P to provide a suitable teaching signal.

are learnt using the covariance learning rule $\delta w_{ij} = -\beta e_i q_j$, where e_i is the difference between the desired and actual output at each step (i) and β is the learning rate.

The cerebellar control scheme is shown in the flow diagram in Figure 2A where the cerebellar filter C is embedded in a recurrent loop. Recurrent connectivity is a characteristic feature of the cerebellum [34], possibly because in this architecture output error is a suitable training signal and no prior model of the inverse plant is required [31]. The brainstem B is an approximate fixed feedforward controller for the plant P. A reference model M is included in the control scheme (an extension to the original computational model of the VOR [26]) so that exact compensation is achieved when $B = MP^{-1}$. The behaviour of the controlled plant then matches that of the reference model M which specifies a realistic response for the controlled plant; the use of a reference model also ensures that the estimated controller is proper [32]. In this contribution the reference model used is defined in continuous time as

$$M = \frac{1}{(\tau s + 1)^n} \tag{2}$$

where $\tau = 0.1$s, and n is the difference between the number of plant poles and zeros.

2.2 Filtered X-LMS Algorithm

The FXLMS algorithm is a feedforward adaptive filter control algorithm widely used for active control applications [16, 33]. A schematic of the control scheme using FXLMS is given in Figure 2B. For the adaptive filter controller C, we used the same bank of α-function filters and bias term as the cerebellar adaptive filter (described above). The filter outputs were again passed through a Q-matrix to decorrelate the signals.

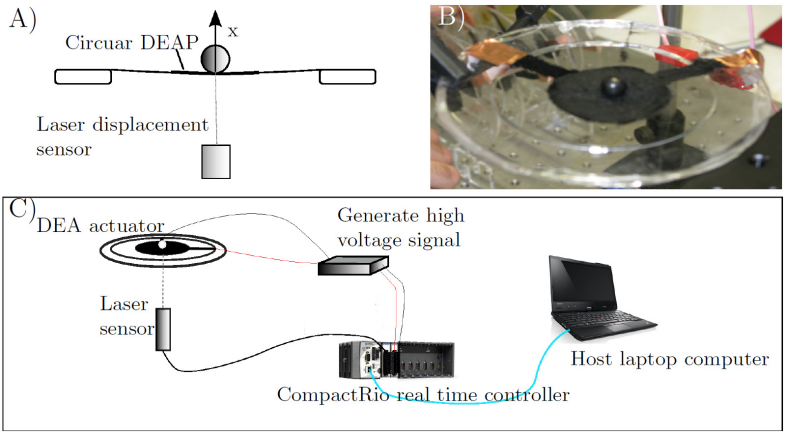

Fig. 3. Summary of the experimental set up. A) A laser displacement sensor is used to measure the vertical displacement of a mass on a circular DEA. B) DEA actuator stretched on circular perspex frame supporting spherical load. C) Summary of experimental real-time control connectivity.

3 Experimental Details

This section details the experimental set-up used to test one degree-of-freedom control of a DEA. Our DEA actuator is comprised of a thin passive elastomer film, sandwiched between two compliant electrodes. In response to an applied voltage the electrodes squeeze the film in the thickness direction, resulting in biaxial expansion. In order to constrain the controlled variable to one degree of freedom a spherical load was placed at the centre of a circular DEA and its motion in the vertical plane (i.e. vertical displacement) was measured. A summary of the experimental setup is provided in Figure 3.

The DEAs are constituted of acrylic elastomer (3M VHB 4905) with an initial thickness of 0.5mm. A conductive layer of carbon grease (MG chemicals) constitutes the capacitor plates. The elastomer was pre-stretched biaxially by 350% (where 100% was the unstretched length) prior to being fixed on a rigid perspex frame with inner and outer diameters of 80mm and 120mm respectively. The electrodes were brushed on both sides of the VHB membrane as circles with a diameter of approximately 35mm. The load used during experiments was a sphere weighing 3g. The control hardware was a CompactRio (CRIO-9014, National Instruments) platform, with input module NI-9144 (National Instruments) and output module NI-9264 (National Instruments) used in combination with a host laptop computer. LabView was run on the host laptop computer, with communication between the host laptop and CompactRio (CRio) carried out using the LabView shared variable engine. This real-time setup enabled accurate timing of control inputs and outputs with input and output signals being sampled simultaneously at 50Hz.

A laser displacement sensor (Keyence LK-G152, repeatability - 0.02mm) was used to measure the vertical movement of the mass sitting on a circular DEA. This signal was supplied to the input module of the CRio. From the output module of the CRio, voltages in the range 1.1V-3.75V were passed through a potentiometer (HA-151A HD Hokuto Denko) and amplified (EMCO F-121 high voltage module) with a ratio of 15V:12kV and applied to the DEA. During the real-time experiments the cerebellar controller (described in the previous section) was used to adjust the voltage input to the DEA to track a desired coloured-noise reference signal. The reference signal was low pass filtered white noise with frequency range 0-1Hz, and the amplitude constrained to 0.2-0.65.

4 Results

This section presents the results for measurement and control of the vertical displacement of the DEA. The results are divided into the following sub-sections: real-time control of the DEA, identification of a model of the plant input-output response, and comparison in simulation of the biomimetic and conventional algorithms.

4.1 Real-Time Control of DEA Using the Biomimetic Algorithm

In this experiment the cerebellar algorithm was applied to real-time control of the DEA actuator. In the experiments described here the reference signal was constrained to lie in the linear range of the plant. The brainstem, B was an approximate feedforward controller, modelled as in Eq. (6) using $0.087, 0.331, -0.317$ for the identified parameters a_0, b_0, c_0 respectively (see below for details of model identification). Initial cerebellar weights were set to zero.

The algorithm was tested for its ability to learn the dynamics in order to track the vertical displacement of the DEA. Figure 4 shows the results from a displacement tracking run. The algorithm quickly learnt the filter weights which allowed accurate tracking and tracking quality remained stable over the length of the experiment. The learning rate was chosen to give robust and stable learning on a time-scale which allowed tracking of variations in model parameters.

4.2 Identifying a Plant Model of the Actuator

A model of the DEA plant was identified to allow detailed comparison of the biomimetic algorithm with a conventional algorithm. This allowed us to use exactly the same data set for both algorithms in control simulations. The fitted model also allowed us to quantify the time dependence of actuator properties. The dynamics of the DEA, and their change over-time, were measured by recording the displacement response (Fig. 5B) to an applied voltage (Fig. 5A) over a 30 minute period. A non-linear dynamic model, with Hammerstein structure, of the response was estimated as

$$a\dot{x} + x = \begin{cases} bu + c, & \text{if } u < e \\ bu + c + d(u-e)^2, & \text{otherwise} \end{cases} \tag{3}$$

where x is the vertical displacement of the EAP, u the voltage input (prior to amplification), and a, b, c, d, and e are the model parameters. These parameters were estimated by fitting to 1 minute of data. An example of the resulting fit is given in Figure 5C. The response characteristics changed over time so model parameters were estimated by fitting to 1min segments of data every 3mins over the 30mins of data. These parameter estimates and a linear least squares fit to their changes over time are shown in Figure 5D. The suitability of this identified model for investigating control performance in simulation is illustrated in Figure 4, where the performance of the cerebellar algorithm in the real-time control situation and in simulation are shown to be very similar.

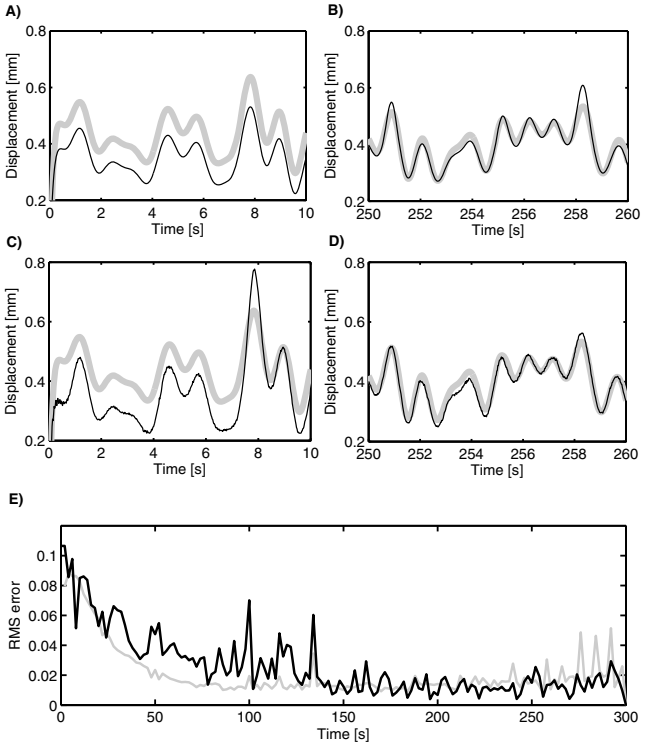

Fig. 4. Experimental adaptive control of DEA using cerebellar-inspired control. Cerebellar weights are initially set to zero and the brainstem is an approximate fixed compensator. A) Desired ( ) and actual ( ) response of simulated plant before learning. B) Desired ( ) and actual ( ) response of simulated plant after learning. C) Desired ( ) and actual ( ) response of experimental plant before learning. D) Desired ( ) and actual ( ) response of experimental plant after learning. E) Windowed rms errors during learning, for simulated ( )and experimental ( ) plants.

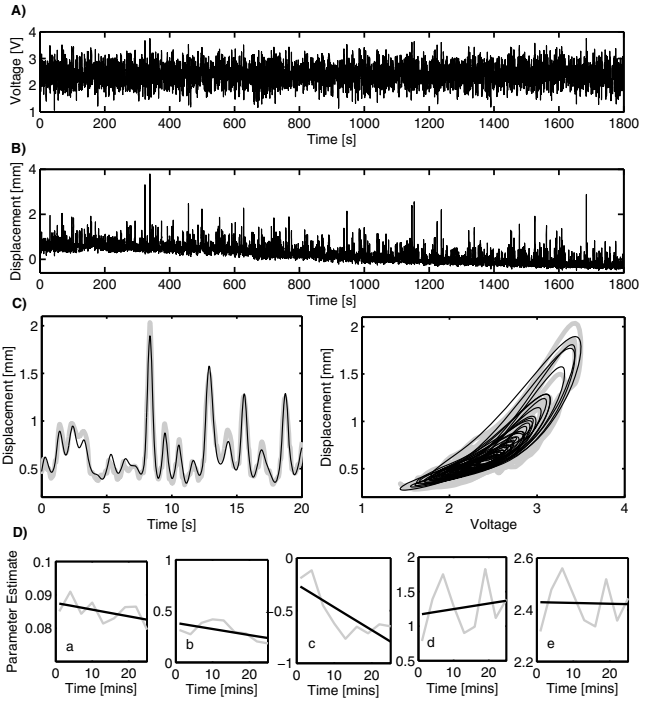

Fig. 5. Dynamic response and dynamic modelling of DEA actuator. A) Voltage input prior to amplification. The voltage input is 0-1Hz band limited white noise, constrained to range from 1.1-3.75V, this is passed through a high voltage amplifier with ratio of 15V:12kV and applied to the DEA. B) Vertical displacement response of a mass on a circular DEA during 30 minutes of actuation. C) Measured (▬) and modelled (▬) vertical displacement, fitting to 60 seconds of data, modelled using Eq. (3). D) Parameters of model given in Eq. (3) (▬) estimated for the 30mins of data. Parameter estimates were updated every 3mins by fitting to 1min of data. The least squares linear fit to the change is parameters over time (▬) is also plotted.

4.3 Control of Simulated DEA Plant

The cerebellar control algorithm was compared to the FXLMS algorithm by applying both to the control of the simulated plant described by the model given in Equation (3), with time varying model parameters

$$\begin{aligned} a(t) &= 0.085 \\ b(t) &= 0.316 - 0.006t \\ c(t) &= -0.193 - 0.020t \\ d(t) &= 0.784 + 0.008t \\ e(t) &= 2.316 \end{aligned} \tag{4}$$

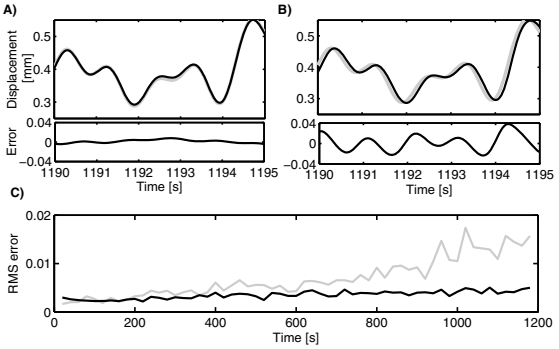

Fig. 6. Simulated adaptive control of EAP actuator using FXLMS and cerebellar-inspired control. A simulated plant based on the model in Eq. (3), with coefficients that vary slowly over time is tracked for 20mins. A) The desired (▬) and actual (▬) displacement response using the cerebellar algorithm, with associated error plotted underneath. B) The desired (▬) and actual (▬) displacement response using the FXLMS algorithm, with associated error plotted underneath. C) Comparison of windowed RMS errors in displacement for the FXLMS algorithm (▬), and the Cerebellar algorithm (▬).

where t is the time in minutes. Initial values are estimated as the fit to the first minute of data, and the gradients in Equations (4) come from the straight line least squares estimates presented in Figure 5D.

The actuator model has nonlinear dynamics (Figure 5C left), so to test the linear cerebellar and FXLMS algorithms described here the reference input was constrained to a range where the plant response was approximately linear. The brainstem B and estimated plant P^* for the cerebellar and FXLMS algorithms respectively were set to the ideal values for a linear approximation of the initial plant model. The input e to output v model describing P^* is

$$a_0\dot{v} + v = b_0 e + c_0 \tag{5}$$

The input (v) to output (u) model describing **B** is

$$\begin{aligned} \tau\dot{u}_t + u_t &= a_0\dot{v} + v \\ u &= (u_t - c_0)/b_0 \end{aligned} \tag{6}$$

where a_0, b_0, c_0 are the parameters given in Equations (4) at time t=0, and τ is the time constant of reference model M. The reference model used is given by Equation (2) with $n = 1$. Initial weights of the adaptive controllers were set to provide optimum compensation for the initial plant. Figure 6 shows the results when tracking the simulated plant for 20mins. Both algorithms are able to accurately track the dynamics of the plant initially, however tracking errors build up over time when using the FXLMS algorithm due to variations in the plant parameters.

5 Discussion

As expected the dynamic characteristics of the DEA show considerable change over time. These changes are likely to be due to creep and highlight the need for a control algorithm capable of compensating for secular changes in the plant dynamics. Although both the FXLMS and cerebellar control algorithms were shown to perform effectively when tracking the simulated plant for a short time period, uncompensated tracking errors eventually developed when using the FXLMS algorithm over a longer period (Fig. 6C). The same increase in error is not seen in the bioinspired cerebellar algorithm. The probable cause of the increasing error when using the FXLMS algorithm is that, over time, the estimated plant model P^* used to provide a suitable teaching signal becomes less accurate, which affects the convergence properties of the learning rule. In contrast the cerebellar algorithm is embedded in a recurrent loop in which output error itself is a suitable training signal [26], meaning an accurate estimate of the plant is not required.

In each algorithm a compact basis (with four filters, plus a bias term) was used to represent a wide range of time scales. This basis provides a biologically plausible way of representing timing. Using a set of basis functions to replace TDLs can also greatly reduce the number of model parameters. In engineering applications Laguerre, or Kautz functions are often used to replace TDLs. They form an orthonormal basis for white noise (as do TDLs), and are insensitive to the sampling frequency (unlike TDLs) [27].

In this contribution we have focused on the control of a DEA over its linear operating range. The cerebellar algorithm could be extended to the control of non-linear systems by including an approximate plant linearization stage in the brainstem, or by using a non-linear adaptive filter which includes non-linear basis, or combining the two schemes.

The presented control task is used to provide a test for the control algorithms. The cerebellar algorithm described here can be applied to generic control tasks. For example, it could be used to control the impedance, or force response. In applications to robotic systems it is likely that the movement of multiple actuators will be coupled (perhaps including agonist-antagonist configurations). It has been show multiple actuators can produce useful behaviours [9]. The recurrent cerebellar control architecture presented here has previously been shown to be well adapted to the control of such multi degree of freedom systems [19].

6 Conclusions

In this investigation we have developed an adaptive control algorithm for DEA actuators inspired by the function of the cerebellum. The adaptive cerebellar-inspired algorithm, in combination with a simple fixed controller, learns to represent the inverse dynamics of the DEA actuator and therefore forms a feed-forward inverse plant compensation control scheme. We have demonstrated the suitability of the cerebellar-inspired algorithm for real-time tracking control of a DEA actuator over its linear range of operation. The cerebellar-inspired control

algorithm successfully adapted to time-variation in the dynamics of the DEA actuator. We further benchmarked the performance of the cerebellar inspired algorithm in simulation, using an identified nonlinear dynamic model of the DEA actuator, against a conventional adaptive control scheme (filtered-XLMS). The cerebellar-inspired scheme was shown to outperform filtered-XLMS over long time periods of operation.

Acknowledgements: This work was supported by EPSRC grant no. EP/IO32533/1, *Bioinspired Control Of Electro-Active Polymers for Next Generation Soft Robots*.

References

1. Carpi, F., Kornbluh, R., Sommer-Larsen, P., Alici, G.: Electroactive polymer actuators as artificial muscles: are they ready for bioinspired applications? Bioinspir. Biomim. 6(4), 045006 (2011)
2. Carpi, F., Raspopovic, S., Frediani, G., De Rossi, D.: Real-time control of dielectric elastomer actuators via bioelectric and biomechanical signals. Polym. Int. 59(3), 422–429 (2009)
3. Van Ham, R., Sugar, T.G., Vanderborght, B., Hollander, K.W., Lefeber, D.: Review of Actuators with Passive Adjustable Compliance/Controllable Stiffness for Robotic Applications. IEEE Robot. Autom. Mag., 81–94 (2009)
4. Bar-Cohen, Y.: Electroactive polymer (EAP) actuators as artificial muscles: reality, potential, and challenges. SPIE Press (2001)
5. Meijer, K., Rosenthal, M.S., Full, R.J.: Muscle-like actuators? A comparison between three electroactive polymers. In: Proc. SPIE, vol. 4329, pp. 7–15 (2001)
6. Xie, S., Ramson, P., Graaf, D., Calius, E., Anderson, I.: An Adaptive Control System for Dielectric Elastomers. In: 2005 IEEE International Conference on Industrial Technology, pp. 335–340 (2005)
7. Pelrine, R., Kornbluh, R.D., Pei, Q., Stanford, S., Oh, S., Eckerle, J., Full, R.J., Rosenthal, M.A., Meijer, K.: Dielectric elastomer artificial muscle actuators: toward biomimetic motion. In: Proc. SPIE, vol. 4695, pp. 126–137 (2002)
8. OHalloran, A., OMalley, F., McHugh, P.: A review on dielectric elastomer actuators, technology, applications, and challenges. J. Appl. Phys. 104(7), 071101 (2008)
9. Conn, A.T., Rossiter, J.: Towards holonomic electro-elastomer actuators with six degrees of freedom. Smart Mater. Struct. 21(3), 035012 (2012)
10. Ozsecen, M.Y., Mavroidis, C.: Nonlinear force control of dielectric electroactive polymer actuators. In: Proc. SPIE, vol. 7642(1) (2010)
11. Hao, L., Li, Z.: Modeling and adaptive inverse control of hysteresis and creep in ionic polymer metal composite actuators. Smart Mater. Struct. 19(2), 025014 (2010)
12. Dong, R., Tan, X.: Modeling and open-loop control of IPMC actuators under changing ambient temperature. Smart Mater. Struct. 21(6), 065014 (2012)
13. Brufau-Penella, J., Tsiakmakis, K., Laopoulos, T., Puig-Vidal, M.: Model reference adaptive control for an ionic polymer metal composite in underwater applications. Smart Mater. Struct. 17(4), 045020 (2008)
14. Yun, K., Kim, W.J.: Microscale position control of an electroactive polymer using an anti-windup scheme. Smart Mater. Struct. 15(4), 924–930 (2006)

15. Sarban, R., Jones, R.W.: Physical model-based active vibration control using a dielectric elastomer actuator. J. Intel. Mat. Syst. Str. 23(4), 473–483 (2012)
16. Widrow, B., Walach, E.: Adaptive Inverse Control A Signal Processing Approach. Reissue edn. John Wiley & Sons, Inc. (2008)
17. Dean, P., Porrill, J., Ekerot, C.F., Jörntell, H.: The cerebellar microcircuit as an adaptive filter: experimental and computational evidence. Nat. Rev. Neurosci. 11(1), 30–43 (2010)
18. Porrill, J., Dean, P., Anderson, S. R.: Adaptive filters and internal models: Multilevel description of cerebellar function. Neural Networks (December 28, 2012), http://dx.doi.org/10.1016/j.neunet.2012.12.005
19. Porrill, J., Dean, P.: Recurrent cerebellar loops simplify adaptive control of redundant and nonlinear motor systems. Neural Computation 19(1), 170–193 (2007)
20. Ito, M.: The Cerebellum and Neural Control New York, Raven (1984)
21. Fujita, M.: Adaptive Filter Model of the Cerebellum. Biol. Cybern. 206, 195–206 (1982)
22. Lenz, A., Anderson, S.R., Pipe, A.G., Melhuish, C., Dean, P., Porrill, J.: Cerebellar-inspired adaptive control of a robot eye actuated by pneumatic artificial muscles. IEEE T. Syst. Man. Cy. B 39(6), 1420–1422 (2009)
23. Miller III, W.T.: Real-Time Application of Neural Networks for Sensor-Based Control of Robots with Vision. IEEE T. Syst. Man. Cyb. 19(4), 825–831 (1989)
24. Spoelstra, J., Arbib, A.A., Schweighofer, N.: Cerebellar adpative control of a biomimetic manipulator. Neurocomputing 26-27, 881–889 (1999)
25. Smagt, P.: van der: Cerebellar control of robot arms. Connection Science 10, 301–320 (1998)
26. Dean, P., Porrill, J., Stone, J.V.: Decorrelation control by the cerebellum achieves oculomotor plant compensation in simulated vestibulo-ocular reflex. Proc. R. Soc. B 269(1503), 1895–1904 (2002)
27. Anderson, S.R., Pearson, M.J., Pipe, A.G., Prescott, T.J., Dean, P., Porrill, J.: Adaptive Cancelation of Self-Generated Sensory Signals in a Whisking Robot. IEEE T. Robot. 26(6), 1065–1076 (2010)
28. Ljung, L.: System Identification - Theory for the User, 2nd edn. Prentice Hall, Upper Saddle River (1999)
29. Schweighofer, N., Doya, K., Lay, F.: Unsupervised Learning of Granule Cell Sparse Codes Enhances Cerebellar Adaptive Control. Neuroscience 103(1), 35–50 (2001)
30. Coenen, O.J.D., Arnold, M.P., Sejnowski, T.J.: Parallel Fiber Coding in the Cerebellum for Life-Long Learning. Auton. Robot. 11, 291–297 (2001)
31. Porrill, J., Dean, P.: Recurrent cerebellar loops simplify adaptive control of redundant and nonlinear motor systems. Neural Comput. 19(1), 170–193 (2007)
32. Sastry, S., Bodson, M.: Adaptive Control Stability, Convergence and Robustness. Prentice Hall, Englewood Cliffs (1989)
33. Elliott, S.J., Nelson, P.A.: Active noise control. IEEE Signal Proc. Mag, 12–35 (1993)
34. Kelly, R.M., Strick, P.L.: Cerebellar loops with motor cortex and prefrontal cortex of a nonhuman primate. Journal of Neuroscience 23(23), 8432–8444 (2003)